Parameter Estimation of Wind Turbines with PMSM using Cubature Kalman Filters

M. A. González-Cagigal, José A. Rosendo-Macías, *Senior Member, IEEE*, and A. Gómez-Expósito, *Fellow, IEEE*

***Abstract*—This paper presents a parameter estimation technique for a variable-speed wind turbine with permanent magnet synchronous generator and back-to-back voltage source converter. The proposed technique applies the cubature Kalman filter for the joint estimation of the system dynamic state and a modified set of parameters from which the original model parameters can be algebraically recovered. To the authors knowledge, this work is the first attempt to apply such an innovative technique to a PMSM detailed estimation model including the control parameters of the voltage source converter.**

***Index Terms*—Cubature Kalman filter, variable-speed wind turbine, direct-drive synchronous generator, back-to-back voltage source converter, parameter estimation.**

I. Introduction

In a decarbonized and more electrified future, power systems must be able to cope with increasing amounts of intermittent renewable energy. Excluding hydro, wind energy is so far the dominant renewable source worldwide, both in terms of production share (5.6%) and cumulative installed power (550 GW), of which only about 20 GW (less than 4%) correspond to offshore farms. This means that there exists a huge growth potential for offshore wind technology, still in its infancy, while the best places for onshore farms are being quickly occupied. The average offshore turbine size in Europe (5.9 MW) has nearly doubled in the last decade and some vendors are already announcing machine designs of over 12 MW rated power [1]. The most promising topology for offshore wind energy is the direct-driven, multi-pole Permanent Magnet Synchronous Machine (PMSM) with fully-rated back-to-back Voltage Source Converters (VSC), a turbine concept which lacks the gearbox.

Among the upcoming technical challenges raised by the massive integration of renewables, the need for wind and PV sources to contribute to ancillary services stands out. These include voltage and frequency regulation, according to increasingly demanding grid codes, provision of synthetic inertia to keep current stability margins, fast response (flexibility) in the presence of more frequent and deeper net demand gradients, etc.

In this context, it is most important for grid operators to adopt accurate enough PMSG-based wind turbine models, including the fast acting VSC, in order to evaluate their dynamic behavior. This involves a detailed knowledge of the associated components and their defining equations. Ultimately, the system state evolution is determined by the parameters involved in those equations, which are therefore crucial for the correct operation and control of a power system with a high penetration of wind power plants.

System parameters are customarily considered constant, even under changing operating conditions. However, when this assumption is not accurate enough, or when the control parameters provided by the manufacturer are suspected to be inaccurate or outdated, a model validation is needed to obtain their values considering the actual operating point. This need has been recognized, for instance, in the US, where the NERC has released reliability guidelines [2] regarding the validation of generator models, including synchronous machines and other inverter-based ones exceeding a certain rated power. NERC suggests two ways for generator model validation and calibration: 1) taking the generator out of service and performing specific tests; 2) measurement-based methods based on disturbance recordings from synchrophasors (PMUs), data loggers, fault recorders, etc. This work lies in the second category.

Dynamic state estimators (DSEs) based on Kalman filters (KFs) have been used for state estimation of power systems with nonlinear dynamics, as proposed in [3], which includes a comparison study. A particular formulation of KF, the so-called unscented KF (UKF) has proven to be reliable and accurate for this particular application [4]. For instance, in [5] a method to deal with disturbances in the system is proposed, whereas [6] includes the system parameters in the estimation process.

The UKF technique has also been applied in state estimation of synchronous generators, [7], and joint state and parameter estimation of these machines, [8]. Regarding wind turbines, [9] studies the application of UKF in fault diagnosis. For this type of machines, [10] uses extended KF (EKF) in the estimation of the electrical parameters of doubly-fed induction generators (DFIGs), while [11] proves that the performance of the UKF is superior to that of the EKF in the parameter estimation of DFIGs.

EKF is also used in different studies on permanent magnets synchronous motors. Rotor initial position is estimated in [12] for a sensorless direct torque controlled machine. Flux-linkage is included in the estimation process in [13] for a vector control and in [14] when demagnetization situations are considered. On these machines, fault detection is necessary for a correct operation of the power system. A method using EKF is established in [15] and [16] for stator winding inter-turn short circuit identification.

A real implementation of the studied estimation techniques requires noninvasive measurements taken from the system considered. In this respect, [17] proposes a temperature estimation for PMSMs using noninvasive Kalman filters.

PMSGs are considered in a number of studies dealing with

EKF. For instance, in [18] an estimation of the rotor speed is performed within a sensorless maximum power point tracker. Control systems without encoder are also considered in [19], where EKF is used to estimate the state variables of a back-to-back converter. Measurements obtained from PMUs are introduced in the EKF algorithm in [20].

A recent formulation of KFs, the so-called cubature Kalman filter (CKF), has shown good performance in problems such as state estimation of synchronous generators [21]. Theoretical aspects of this formulation are addressed in [22], where some limitations of other KF schemes, such as UKF, which are not suffered by the CKF, are highlighted. Joint state and parameter estimation using CKF is studied in [23], applied to a vehicle model, and in [24], with permanent magnet synchronous motors.

This work considers a variable-speed PMSM wind turbine, connected to the grid through a back-to-back pair of VSCs, which is capable of controlling its active and reactive power within specified limits. Based on measurement snapshots taken at the point of connection, the state and parameters of the wind turbine and the VSC are jointly estimated using CKF.

This work is organized as follows. Section 2 formulates the equations used in the proposed CKF algorithm. Section 3 analyzes the modeling system under study, with the wind turbine, the synchronous generator and the back-to-back voltage source converter (VSC). The implementation of the CKF is described in Section 4. Section 5 presents simulation results corresponding to the base case and several scenarios facing different disturbances. Section 6 includes a comparison of the performance presented by the CKF estimation technique when increasing measurement and model errors are considered. Finally, the conclusions obtained are presented in Section 7.

II. Cubature Kalman Filter

Kalman Filter implementations require a set of state equations, including the dynamic and the measurement equations. In the case of continuous-time, discrete-measurement non-linear systems, these equations can be expressed as

$$\dot{x}(t) = f(x(t), u(t)) + w(t) \tag{1}$$

$$z(t_k) = g(x(t_k), u(t_k)) + v(t_k) \tag{2}$$

where $x(t)$ is the state vector, $u(t)$ the system input, and $z(t_k)$ the available measurements at instant t_k. The model and measurement noises, $w(t)$ and $v(t_k)$, are assumed to be Gaussian processes with covariance matrices Q and R, respectively.

Considering a time step Δt, the above equations have the following discrete counterparts:

$$x_k = x_{k-1} + \Delta t \cdot f(x_{k-1}, u_{k-1}) + w_k \tag{3}$$

$$z_k = g(x_k, u_k) + v_k \tag{4}$$

which are more appropriate for non-linear Kalman filtering techniques, such as the CKF. This involves an iterative process composed of two different stages, as follows [25].

A. Time Update

At each time k, an estimated state vector $\hat{x}_{k-1}$ of size L, along with the covariance matrix associated to its estimation error, P_{k-1}, are available from the previous step. On the basis of these values, a set of $2L$ cubature points are calculated as follows:

$$S_{k-1} S_{k-1}^T = P_{k-1} \tag{5}$$

$$x_{k-1}^i = S_{k-1} \xi_i \sqrt{L} + \hat{x}_{k-1} \quad i = 1, ..., 2L \tag{6}$$

where S is a positive-definite square root of matrix P (in this paper the Cholesky factorization of matrix P will be used), and ξ_i is the i^{th} cubature node, obtained as the intersection of the unit sphere and the $\mathbb{R}^L$ axis. Compared to other KF formulations, the cubature points are less prone than the σ-points calculated in the UKF to numerical inaccuracy or filter instability, [22]. This issue is further discussed in section V.

The state function $f(\cdot)$ in (3) is evaluated at these cubature points, yielding a set of $2L$ vectors x_k^{i-}, from which an *a priori* estimation of $\hat{x}_k^-$ and P_k^- is in turn computed as follows:

$$\hat{x}_k^- = \frac{1}{2L} \sum_{i=1}^{2L} x_k^{i-} \tag{7}$$

$$P_k^- = \frac{1}{2L} \sum_{i=1}^{2L} x_k^{i-} x_k^{i-T} - \hat{x}_k^- \hat{x}_k^{-T} + Q_k \tag{8}$$

B. Measurement Update

Once the *a priori* estimation is obtained, the covariance matrix P_k^- is factorized in order to calculate the matrix S_k^-,

$$S_k^- S_{k-1}^{-T} = P_k^- \tag{9}$$

and a new set of $2L$ cubature points,

$$x_k^{i-} = S_k^- \xi_i \sqrt{L} + \hat{x}_k^- \qquad i = 1, ..., 2L \tag{10}$$

at which function $g(\cdot)$ in (4) is evaluated, yielding:

$$\gamma_k^{i-} = g(x_k^{i-}, u_k) \qquad i = 1, ..., 2L \tag{11}$$

Then the measurement estimation, $\hat{z}_k^-$, its covariance matrix, P_{zk}^-, and the cross-covariance matrix of state and measurements, P_{xzk}^-, are calculated as follows:

$$\hat{z}_k^- = \frac{1}{2L} \sum_{i=1}^{2L} \gamma_k^{i-} \tag{12}$$

$$P_{zk}^- = \frac{1}{2L} \sum_{i=1}^{2L} \gamma_k^{i-} \gamma_k^{i-T} - \hat{z}_k^- \hat{z}_k^{-T} + R_k \tag{13}$$

$$P_{xzk}^- = \frac{1}{2L} \sum_{i=1}^{2L} x_k^{i-} \gamma_k^{i-T} - \hat{x}_k^- \hat{z}_k^{-T} \tag{14}$$

allowing the cubature Kalman gain to be obtained from,

$$K_k = P_{xzk}^- (P_{zk}^-)^{-1} \tag{15}$$

Finally, the *a posteriori* predictions of the state vector, $\hat{x}_k$, and the covariance P_k are obtained as

$$\hat{x}_k = \hat{x}_k^- + K_k (z_k - \hat{z}_k) \tag{16}$$

$$P_k = P_k^- - K_k P_{zk}^- K_k^T \tag{17}$$

which enter the next iteration of the algorithm.

III. System modeling

This section presents the equations describing the dynamics of the system under study, composed of the wind turbine with pitch angle control, the synchronous generator and the back-to-back VSC (Figure 1).

A. Wind Turbine

The mechanical power produced by the turbine at wind speed v_w is given by, [26]:

$$p_w = \frac{1}{2S_n} c_p(\lambda) \pi R^2 v_w^3 \tag{18}$$

where R is the rotor radius, S_n the system rated power and $c_p(\lambda)$ the performance coefficient. For a turbine model with control of the pitch angle, θ_p, and a given tip speed ratio, λ, this coefficient is obtained from,

$$c_p(\lambda) = 0.22 \left(\frac{116}{\lambda_i} - 0.04\theta_p - 5 \right) e^{-\frac{12.5}{\lambda_i}} \tag{19}$$

where

$$\frac{1}{\lambda_i} = \frac{1}{\lambda + 0.08\theta_p} - \frac{0.035}{\theta_p^3 + 1} \tag{20}$$

$$\lambda = \frac{2\omega R}{n_{pole} v_w} \tag{21}$$

ω is the shaft angular speed and n_{pole} is the number of poles of the generator.

The pitch angle control is aimed at maximizing the power production for a specified angular speed. In this work, the following optimal power, p_w^{opt}, characteristic for each wind turbine, is considered,

$$p_w^{opt} = \begin{cases} 0 & \text{if} \quad \omega < 0 \\ 2\omega - 1 & \text{if} \quad 0 \leq \omega \leq 1 \\ 1 & \text{if} \quad \omega > 1 \end{cases} \tag{22}$$

while the control of θ_p is represented with first order dynamics:

$$\dot{\theta}_p = \frac{1}{T_p} \left(K_p(\omega - \omega^{ref}) - \theta_p \right) \tag{23}$$

ω^{ref} being the reference angular speed.

To connect the turbine and the generator, a rigid shaft is considered, so that the equation describing the angular speed dynamics can be expressed as follows:

$$\dot{\omega} = \frac{1}{2H_{tm}} \left(\frac{p_m - p_e}{\omega} \right) \tag{24}$$

where p_e is the electric power comsumption.

Equations (23)-(24) include a set of dynamic parameters, listed in Table I, whose values are unknown. The goal of this work is to estimate those parameters using a CKF.

Table I
Wind Turbine parameters

Symbol	Parameter
T_p	Pitch angle control Time Constant
K_p	Pitch angle control Gain
H_{tm}	Turbine-rotor inertia constant

B. Synchronous Generator

In this work, a permanent magnet synchronous generator is considered, where the voltage (v_s), and current (i_s), at the machine terminals are related through the electromagnetic equations in dq axis, [26],

$$v_{sd} = \omega L_q i_{sq} \tag{25}$$

$$v_{sq} = -\omega(L_d i_{sd} - \psi_p) \tag{26}$$

L_d and L_q being the generator inductances in dq axis, and ψ_p the rotor permanent field flux.

These magnitudes are used to calculate the active and reactive power delivered by the synchronous generator,

$$p_s = v_{sd} i_{sd} + v_{sq} i_{sq} \tag{27}$$

$$q_s = v_{sq} i_{sd} - v_{sd} i_{sq} \tag{28}$$

As the machine is supposed to be rigidly connected to the turbine, p_s replaces p_e in equation (24).

In this work, the value of the generator inductances, L_d and L_q, which can be obtained with different factory tests, are assumed to be known and therefore are not included in the parameter estimation problem.

C. Back-to-back VSC

The converter allows controlling the active power and either the reactive power produced by the generator or the voltage at the VSC external bus. The control variables are the currents on the VSC generator and grid sides, i_s and i_c, respectively, in $d-q$ axis. The dynamic equations are represented as follows [26]:

$$\frac{di_{sq}}{dt} = \frac{1}{T_{qs}} \left(\frac{p_w^{opt}}{\omega(\psi_p - L_d i_{sd})} - i_{sq} \right) \tag{29}$$

$$\frac{di_{sd}}{dt} = \frac{1}{T_{ds}} \left(K_{ds}(q_{s0} - q_s) - i_{sd} \right) \tag{30}$$

$$\frac{di_{cq}}{dt} = K_{qc}(p_s - p_c) \tag{31}$$

$$\frac{di_{cd}}{dt} = \frac{1}{T_{dc}} \left(K_{dc}(v^{ref} - v_h) - i_{cd} \right) \tag{32}$$

Table II collects the parameters of the converter to be estimated using CKF.

Equations (29) - (32) represent the VSC model as implemented by the CKF algorithm, which constitutes a simplification of the simulation model adopted for the sole purpose of obtaining measured magnitudes, [28]. This latter model

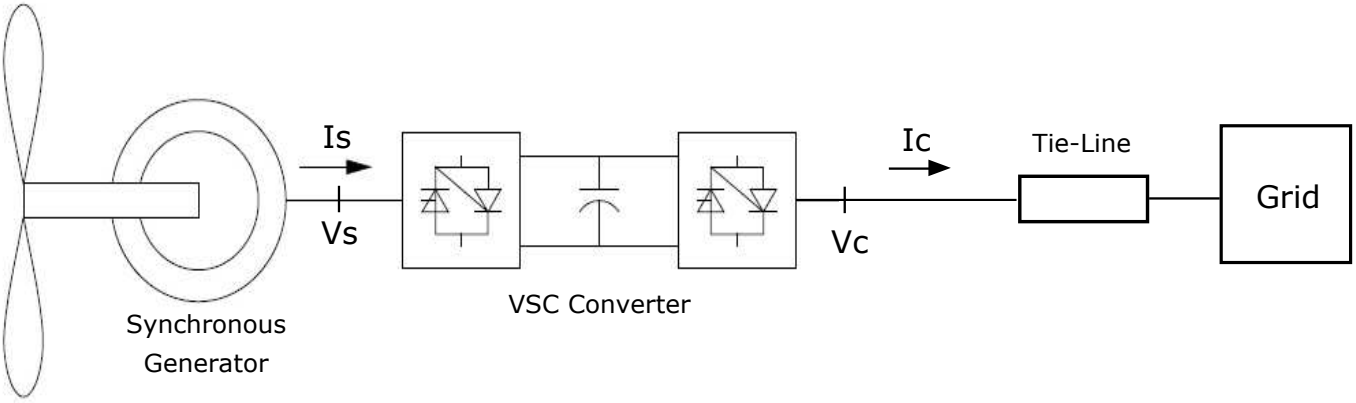

Figure 1. Components of the simplified system under study.

includes other components which are present in real wind power plants, such as the AC filter and the DC-link voltage controller, so that the measurements used in the estimation process are as close as possible to those that would be captured from the actual system.

Table II
BACK-TO-BACK VSC PARAMETERS

Symbol	Parameter
T_{qs}	Generator side q-axis Time Constant
K_{ds}	Generator side d-axis Gain
T_{ds}	Generator side d-axis Time Constant
K_{qc}	Grid side q-axis Gain
K_{dc}	Grid side d-axis Gain
T_{dc}	Grid side d-axis Time Constant

IV. IMPLEMENTATION OF THE CKF

In the previous section, the parameters involved in the dynamic model (18)-(32) have been presented. As most of those parameters are not precisely known, or are simply unknown, they should be included in an augmented state vector for a joint state-parameter estimation using CKF.

An initial attempt to estimate the original raw parameters was unsuccessful, owing to convergence problems. Therefore, a parameter modification technique is proposed, similar to the one adopted in [27] for synchronous machine parameter estimation. With this technique, the augmented state vector becomes $x_a^T = [x^T, \psi^T]$, where the state vector, x, contains the following state variables,

$$x^T = [i_{sd}, i_{sq}, \omega, \theta_p, i_{cd}, i_{cq}]$$

and ψ is the modified parameter vector, as proposed in this work,

$$\psi^T = [\frac{10}{H_{tm}}, \frac{K_{qc}}{10}, \frac{1}{T_{dc}}, K_{dc}, \frac{1}{T_{ds}}, \frac{1}{T_{qs}}, K_{ds}, \frac{1}{T_p}, K_p]$$

Therefore, the size of the augmented vector is $L = 15$.

Equations (3) and (4) can be rewritten in terms of x_a and an augmented-model noise vector, w_k, involving the state and parameter components, yielding:

$$\begin{bmatrix} x_k \\ \psi_k \end{bmatrix} = \begin{bmatrix} x_{k-1} + \Delta t \cdot f(x_{k-1}, u_{k-1}) \\ \psi_{k-1} \end{bmatrix} + w_k \quad (33)$$

$$z_k = g(x_{ak}, u_k) + v_k \quad (34)$$

Regarding the measurement update stage in the CKF algorithm, seven easily measurable magnitudes are considered: the magnitude and phase angle of the voltage (V, θ_V) and current (I, θ_I) at the VSC external bus, which can be provided by a PMU unit, the shaft angular speed ω, the pitch angle θ_p and the wind speed v_w. In turn, it is customary to divide this set into inputs, $u^T = [v_w, V, \theta_V]$, and measurements, $z^T = [\omega, I, \theta_I, \theta_p]$, [29].

Then, the function $g(x_{ak}, u_k)$ in (34) reduces in this case to,

$$I = \sqrt{i_{cd}^2 + i_{cq}^2} \quad (35)$$

$$\theta_I = \arctan\left(\frac{i_{cd}}{i_{cq}}\right) \quad (36)$$

Note that ω and θ_p lead to trivial expressions, as they are state variables.

V. CASE STUDIES

In this section, the results of three performance tests are presented to confirm the accuracy and robustness of the proposed estimation method, when the reduced power system shown in Figure 1 faces different disturbances. The magnitudes defining the steady-state starting point (v^{ref} and ω^{ref}) are obtained by assuming an initial complex power injection at the connection point ($S_c = 0.7 + j0.5pu$), the base power being equal to the rated power of the wind turbine ($S_B = 2MW$). The simulations have been carried out using Matlab Simulink. Note that the simulation model considered for the generation of exact magnitudes, [26], is more detailed and accurate than that adopted by the CKF algorithm. Specifically, the stator resistance and a set of control parameters involved in the VSC and the pitch angle control, are neglected in the CKF system model described in section III. This is intentionally done in order to consider the more realistic situation in which

the model assumed by the CKF does not necessarily reflect the exact model, but a simplified one.

The exact parameter values adopted in the simulation are listed in Table III, excluding those that are not considered in the estimation process, such as the stator resistance. The time step for the simulations and the CKF process is $\Delta t = 0.01s$.

Table III
EXACT PARAMETER VALUES

Parameter	Unit	Exact Value
H_{tm}	s	4
K_{qc}	pu	35
T_{dc}	s	0.5
K_{dc}	pu	1.5
T_{ds}	s	0.5
T_{qs}	s	0.5
K_{ds}	pu	1.5
T_p	s	3
K_p	pu	2

The CKF estimator requires an initial state for x_a. For the state variables, x, an initialization process is used, based on the steady-state point [30], leading to the initial values shown in Table IV.

Table IV
INITIAL VALUES FOR THE STATE VARIABLES

Variable	Initial Value
i_{sd}	1
i_{sq}	1.07
ω	0.7
θ_p	0
i_{cd}	0.4
i_{cd}	0.75

In order to test worst case conditions, regarding the accuracy of the available parameter values (from manufacturer data, similar machines or other sources), the proposed modified parameter vector, ψ, is initialized with a random value in the range $\pm 30\% \div \pm 50\%$ of their real values. This way, the proposed estimation technique becomes a method for the validation of the parameter values.

The initial covariance of the state estimation error is defined as a diagonal matrix,

$$P_0 = diag([P_{x0}^T, P_{\psi 0}^T])$$

where

$$P_{x0}^T = [10^{-4}, 10^{-4}, 10^{-4}, 10^{-4}, 10^{-4}, 10^{-4}]$$

corresponds to the state variables, and

$$P_{\psi 0}^T = [1, 1, 1, 1, 1, 1, 1, 1, 1]$$

to the modified parameters.

The covariance matrix Q has been assumed as a diagonal matrix with $Q_{ii} = 10^{-8}$, while the covariance matrix R has been taken as a diagonal matrix with $R_{ii} = 10^{-4}$, corresponding to an error with 1% s.d. (lower accuracy than that typically provided by PMUs).

A. *Base case: smooth operating point variations*

In this scenario, the impedance of the line connecting the PMSM generator to the infinite busbar is $z_L = 0.01 + j0.1$ pu. The magnitude and angle of the busbar voltage evolve as Gaussian random walks with standard deviation $R_w = 10^{-4}$, as represented in Figure 2.

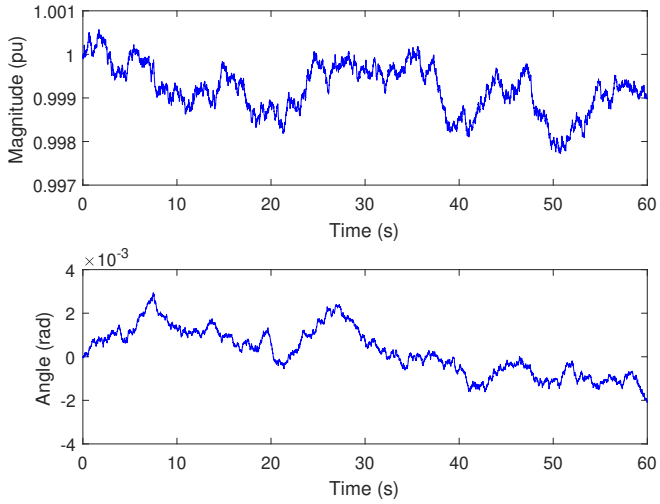

Figure 2. Gaussian random walks applied to the connection point bus voltage

The system under study is supposed to be in normal operating conditions. The evolution considered for the wind speed, v_w, is taken at a mean value of 16 m/s with a standard deviation of 10^{-2} simulating the real variability, [31]. This signal (Figure 3), is used as an input for the CKF algorithm.

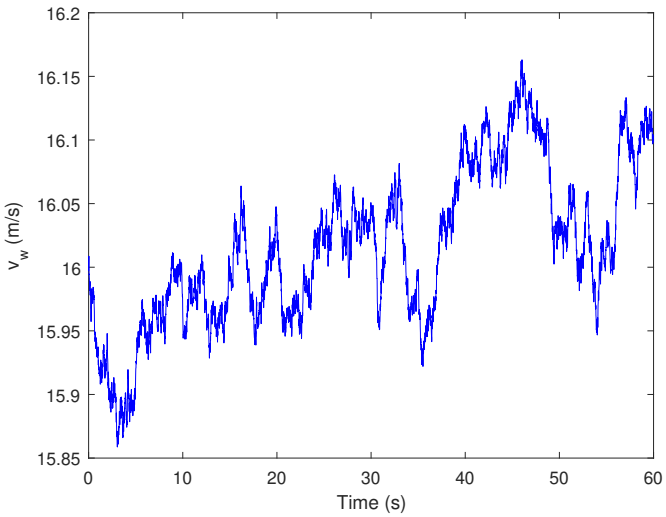

Figure 3. Wind speed evolution for the base case scenario

The estimation technique proposed in this work has proven to be accurate when small and random variations of the operating point are considered. Figure 4 shows the results of the CKF estimation process throughout 60s for the modified parameter representing the turbine-motor inertia constant H_{tm},

while the VSC and the pitch angle control parameters are represented in Figure 5. For each parameter, the estimated value, $\hat{x}_i$, is represented along with the $\hat{x}_i \pm 3S_{ii}$ bounds. Note that the covariances tend to Q_{ii}, showing the accuracy of the converged estimation.

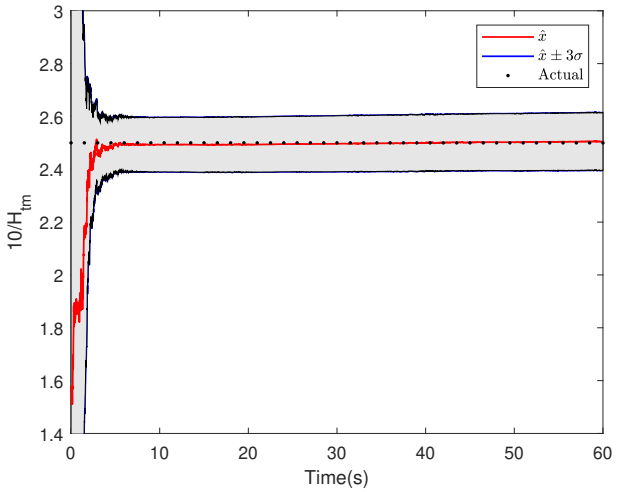

Figure 4. Estimation result for the turbine-motor inertia constant

As can be seen, the method eventually converges to the neighborhood of the correct modified parameters, from which the original parameters can be recovered, as per equations (18)-(32). The estimated value of the original parameters and the relative estimation error are summarized in Table V. Note that the largest relative error is 2.1%.

Table V
RELATIVE ERROR IN PARAMETER ESTIMATION WITH SMOOTH VARIATIONS

Parameter	Estimated Value	Relative Error (%)
H_{tm}	4.012	0.300
K_{qc}	34.426	1.640
T_{dc}	0.503	0.600
K_{dc}	1.513	0.867
T_{ds}	0.504	0.800
T_{qs}	0.511	2.100
K_{ds}	1.510	0.667
T_p	2.991	0.300
K_p	2.023	1.150

The performance of the proposed estimation technique, based on CKF, has been compared with that shown by other KF filter schemes, such as UKF and EKF, as illustrated in Figure 6, where the estimation of the shaft inertia under soft variations in the system is shown. Note that the EKF provides an unacceptable estimated value for the modified parameter and that the UKF presents convergence problems in the long term.

Once the accuracy of the parameter estimation process has been shown under mild operating conditions, the robustness of the proposed estimation technique is tested with three large disturbances separately arising in the system under study.

B. Disturbance 1: wind gust

This test considers an abrupt change in the wind speed, which is modeled as a *Mexican Hat Wavelet* [31], as shown in Figure 7.

The evolution of the voltage at the point of connection is the same as in the base case.

In this case, the parameters are initialized with their estimated values, as provided by the base case. As the initial estimation is more accurate, the elements of $P_{\psi 0}$ are reduced to 10^{-4}. The value of Q_{ii} has also been modified to 10^{-6}.

The estimated parameters showed no significant variations during the wind gust, reaching the same values as in the base case after a small transient, once the disturbance vanishes. As an example, the evolution of $10/H_{tm}$ is provided in Figure 8, where a zoomed view is added to better visualize the transient behavior.

C. Disturbance 2: Voltage dip

The second disturbance considered is a 70% voltage dip at the point of connection that elapses for 1s (Figure 9). The tie-line impedance and the standard deviation of the Gaussian random walks are the same as in the previous case. The wind speed is assumed to remain as in the base case.

The initial estimation for the parameters and the elements of $P_{\psi 0}$ and Q remain the same as in the previous case (Disturbance 1).

Except for a small transient arising during the disturbance, the modified parameters showed no significant variations in the presence of the voltage dip, reaching the same estimated values as in the base case. As an example, the evolution of $1/T_{dc}$ in shown in Figure 10, where the transient behavior can be noticed in the zoomed view.

D. Disturbance 3: Topological change

In the last case study considered in this work, an abrupt variation in the tie-line impedance is assumed, representing a sudden topological change in the external system. For this purpose, at instant $t = 20s$, the value of z_L is modified to $z_L = 0.01 + j0.5pu$ permanently. The value of the voltage at the connection point and the wind speed remain the same as in the base case.

The initial estimation for the parameters and the elements of the matrices $P_{\psi 0}$ and Q remain the same as in the disturbances 1 and 2.

As the disturbance considered in this case is permanent, the estimated values are slightly different to those prior to the disturbance. See the evolution of $1/T_p$ in Figure 11 as an example, where the scale of the transient period is augmented. Note that the accuracy of the estimated parameter in this case has improved minimally.

VI. MEASUREMENT AND MODEL ERROR IMPACT

Once the accuracy of the proposed estimation technique has been proved, the influence of the measurement error on the CKF performance is tested. For this purpose, the smooth system perturbations considered in the base case are

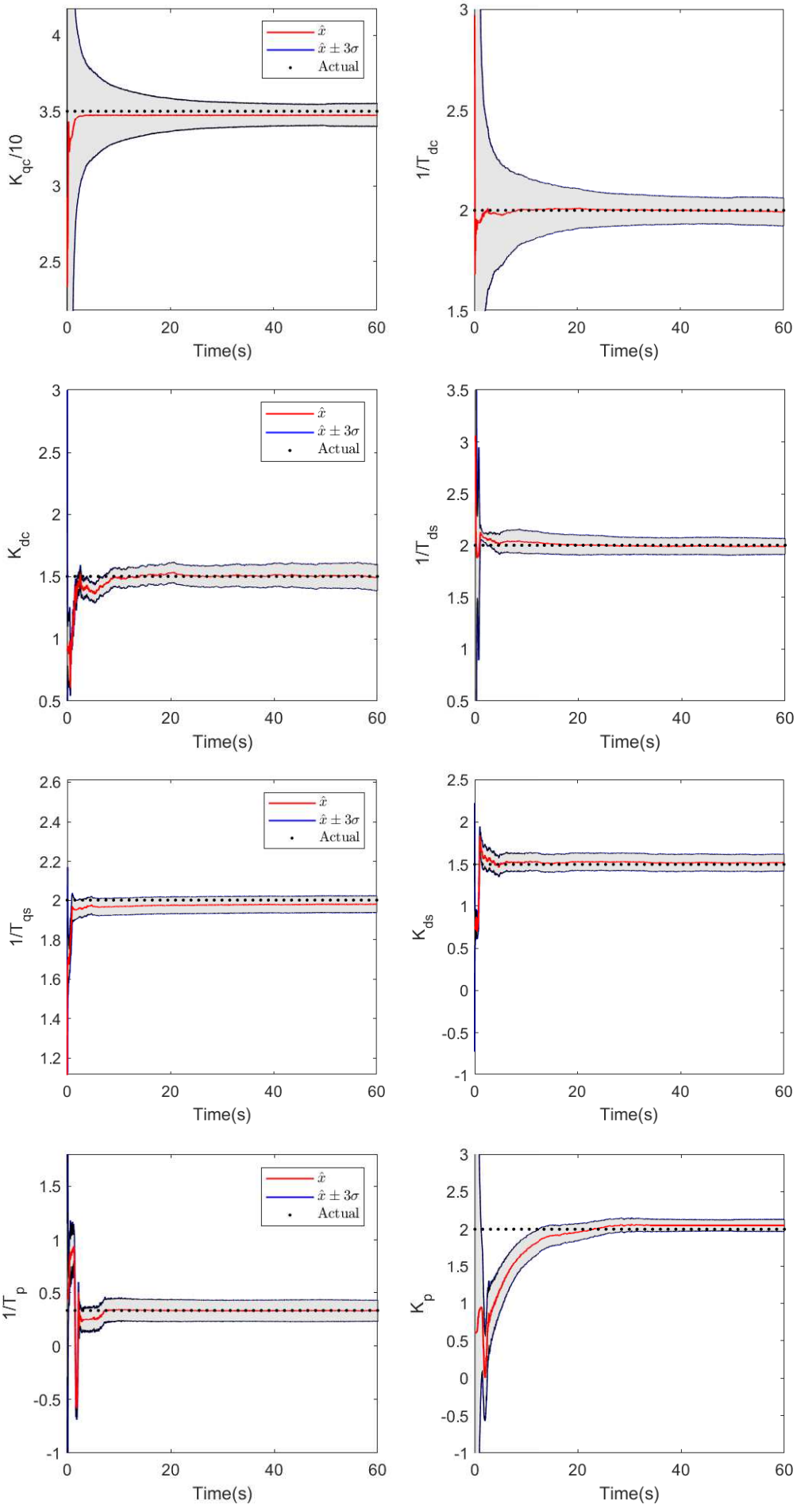

Figure 5. Estimated parameters for VSC and pitch angle control with smooth variations

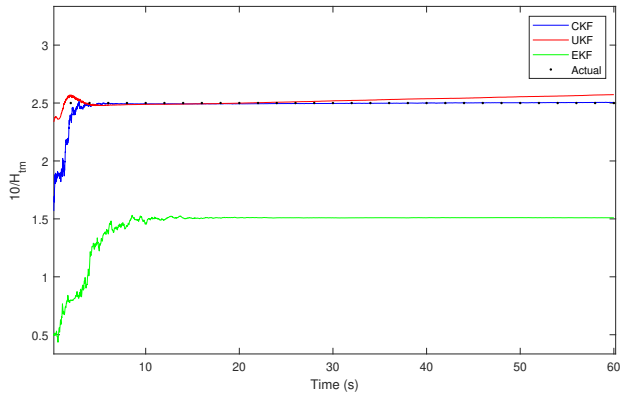

Figure 6. Performance comparison in the estimation of shaft inertia by CKF, UKF and EKF

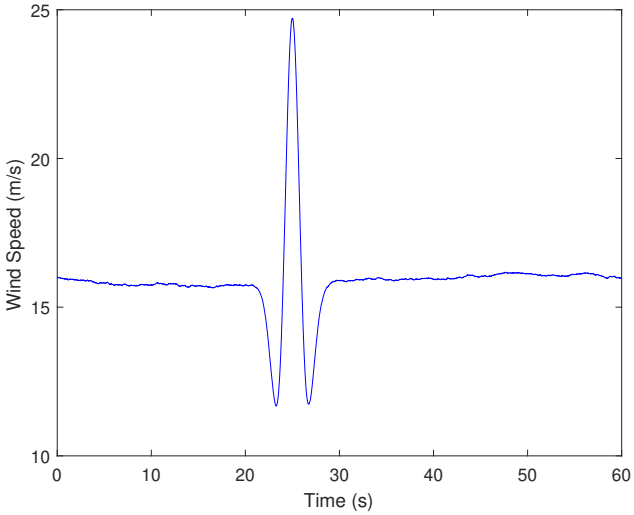

Figure 7. Representation of the *Mexican Hat Wavelet*

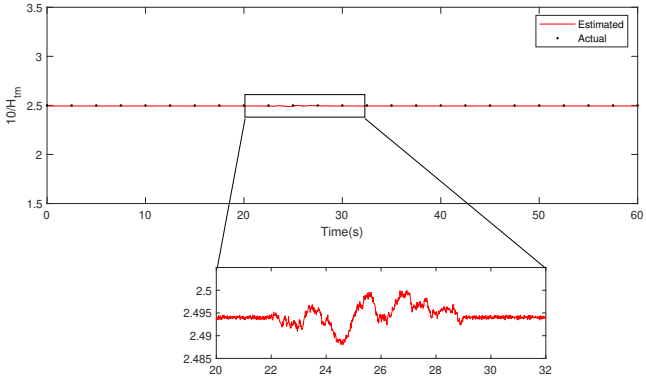

Figure 8. Estimation result for $10/H_{tm}$ with wind gust

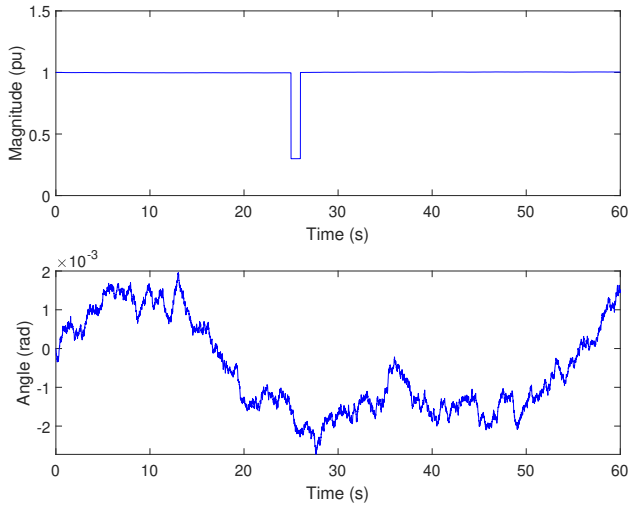

Figure 9. Voltage dip at the point of connection

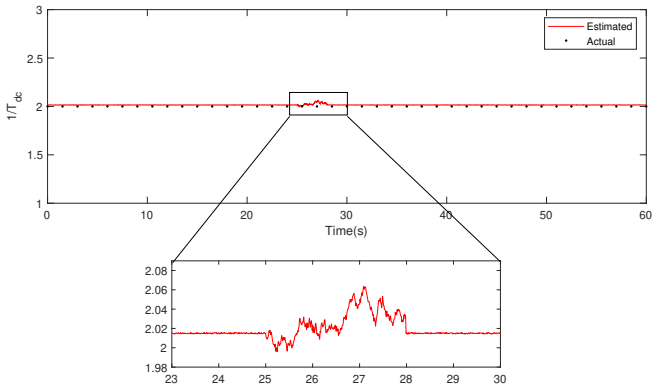

Figure 10. Estimation result for $1/T_{dc}$ with voltage dip

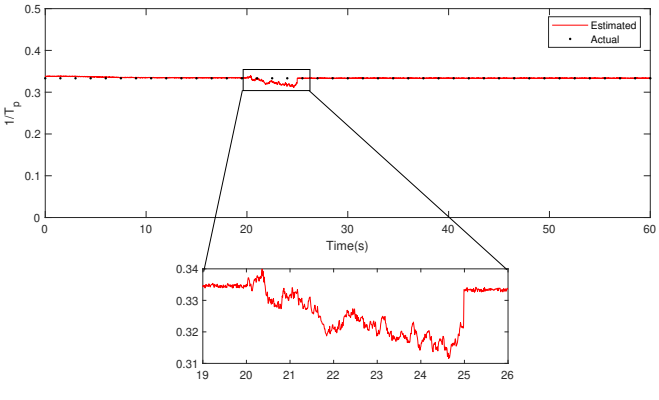

Figure 11. Estimation result for K_p with topological change

repeated by gradually increasing the s.d. of the measurement errors. Table VI summarizes the results obtained in terms of maximum relative error in the parameter estimation. As expected, the lower the measurement accuracy the poorer the estimation results. Note that, if PMUs are used as the source of measurements, with errors typically lower than 1%, then the maximum parameter error will be less than 2%.

On the other hand, the synchronous generator model presented in section III, as given by (25) and (26), includes

Table VI
MAXIMUM RELATIVE PARAMETER ERROR FOR INCREASING MEASUREMENT ERRORS

Measurement error	$\lvert E_r^{max}\rvert(\%)$
1%	2.100
3%	2.854
5%	5.926
7%	10.800

the generator inductances in dq axis, L_d and L_q, which are considered to be known for the CKF implementation. The performance of the estimator with increasing error in those parameters is compared in Table VII, where the variation of the maximum relative error is shown.

Table VII
MAXIMUM RELATIVE PARAMETER ERROR FOR INCREASING ERRORS IN L_d AND L_q VALUES

Model error	$\lvert E_r^{max}\rvert(\%)$
2%	2.107
5%	3.011
10%	6.667
15%	12.002

Note that, while low model errors lead to sufficiently accurate estimation results, when the errors in the known system parameters are large enough, the CKF-based estimator performance deteriorates, in proportion to those errors.

VII. CONCLUSIONS

In this paper, a CKF is used to perform a joint estimation of the state variables and parameters of a variable-speed wind turbine with a direct-drive synchronous generator and a back-to-back VSC.

The proposed method includes a set of modified parameters, providing accurate estimation results (2.1% maximum relative error) under normal small variations in the operating point. A comparison of three KF schemes (CKF, UKF and EKF) has shown that the CKF is the most suitable for the parameter estimation of the system under study.

The robustness of the technique has been successfully proven with three different performance tests, simulating typical large disturbances that can occur in real life. Finally, the results provided by the CKF, for increasing values of measurement errors, show that the estimator performance is acceptable as long as the quality of the measurements remains within a range typically achieved by existing synchrophasors.

ACKNOWLEDGEMENT

The authors would like to acknowledge the financial support of the Spanish Ministry of Economy and Competitiveness under grant PCIN-2015-043 and the Ministry of Education and Professional Training under grant FPU17/06380.

REFERENCES

[1] Offshore Wind in Europe: Key trends and statistics 2017, European Wind Energy Association (EWEA). https://windeurope.org/wp-content/uploads/files/about-wind/statistics/WindEurope-Annual-Offshore-Statistics-2017.pdf

[2] NERC, "Reliability Guideline: Power Plant Dynamic Model Verification using PMUs", 2016. Downloadable from: https://www.nerc.com/comm/PC_Reliability_Guidelines_DL/Reliability%20Guideline%20-%20Power%20Plant%20Model%20Verification%20using%20PMUs%20-%20Resp.pdf

[3] Zhenyu Huang, Kevin Schneider and Jarek Nieplocha,"Feasibility studies of applying Kalman Filter techniques to power system dynamic state estimation", in: International Power Engineering Conference (IPEC), Dec. 2007.

[4] A. Kumar and Bikash C. Pal, "Dynamic Estimation and Control of Power Systems". ISBN: 978-0-12-814005-5. Academic Press edition, October 2018.

[5] J. Zhao and L. Mili, "A Robust Generalized-Maximum Likelihood Unscented Kalman Filter for Power System Dynamic State Estimation" in IEEE Journal of Selected Topics in Signal Processing, vol. 12, no. 4, pp. 578-592, Aug. 2018.

[6] A. Rouhani and A. Abur, "Constrained Iterated Unscented Kalman Filter for Dynamic State and Parameter Estimation" in IEEE Transactions on Power Systems, vol. PP, no. 99, pp. 1-1.

[7] S. Wang, W. Gao, A.P. Sakis Meliopoulos, "An alternative method for power system dynamic state estimation based on unscented transform," IEEE Trans. Power Syst. 27, May 2012.

[8] M.A. González-Cagigal, J.A. Rosendo-Macías, A. Gómez-Expósito, "Parameter estimation of fully regulated synchronous generators using Unscented Kalman Filters", in: Electric Power Systems Research, Volume 168, 2019, Pages 210-217, November, 2018.

[9] Cao Mengnan, Qiu Yingning, Feng Yanhui, Wang Hao and David Infield, "Wind turbine fault diagnosis based on unscented Kalman Filter", in: International Conference on Renewable Power Generation, Oct. 2015.

[10] Mohamed Abdelrahem, Christoph Hackl and Ralph Kennel, "Application of extended Kalman filter to parameter estimation of doubly-fed induction generators in variable-speed wind turbine systems", in: International Conference on Clean Electrical Power (ICCEP), June 2015.

[11] Sahar Pirooz Azad and Joseph Euzebe Tate, "Parameter estimation of doubly fed induction generator driven by wind turbine", in: IEEE/PES Power Systems Conference and Exposition, March 2011.

[12] Qi Jilong, Tian Yantao, Gong Yimin and Zhucheng, "A sensorless initial rotor position estimation scheme and an Extended Kalman Filter observer for the direct torque controlled Permanent Magnet Synchronous Motor Drive", in: International Conference on Electrical Machines and Systems, Oct. 2008.

[13] Xiaoliang Jiang, Pindong Sun and Z.Q. Zhu, "Modeling and simulation of parameter identification for PMSM based on EKF", in: International Conference on Computer, Mechatronics, Control and Electronic Engineering, Aug. 2010.

[14] Xi Xiao and Changming Chen, "Reduction of Torque Ripple Due to Demagnetization in PMSM Using Current Compensation", in: IEEE Transactions on Applied Superconductivity, Volume: 20 , Issue: 3 , June 2010.

[15] Lukas Otava and Ludek Buchta, "Permanent magnet synchronous motor stator winding fault detection", in: IECON 2016 - 42nd Annual Conference of the IEEE Industrial Electronics Society, Oct. 2016.

[16] Lukas Otava and Ludek Buchta, "Implementation and verification of the PMSM stator interturn short fault detection algorithm", in: 19th European Conference on Power Electronics and Applications, Sept. 2017.

[17] Feng, Guodong; Lai, Chunyan; Tjong, Jimi and Kar, Narayan, "Non-invasive Kalman Filter based Permanent Magnet Temperature Estimation for Permanent Magnet Synchronous Machines", in: IEEE Transactions on Power Electronics. PP. 1-1. 10.1109/TPEL.2018.2808323. Feb. 2018.

[18] A. Echchaachouai, S. Elhani, A. Hammouch, S. Guedira,"Extended Kalman filter used to estimate speed rotation for sensorless MPPT of wind conversion chain based on a PMSG", in: 1st International Conference on Electrical and Information Technologies proceedings, pp. 172-177, July 2015.

[19] Zhenbin Zhang, Fengxiang Wang, Guangye Si, Ralph Kennel, "Predictive Encoderless Control of Back-to-Back Converter PMSG Wind Turbine Systems with Extended Kalman Filter", in: IEEE 2nd Annual Southern Power Electronics Conference (SPEC), pp. 1-6, Dec. 2016.

[20] S. A. A. Shahriari, M. Raoofat, M. Mohammadi, M. Dehghani, and M. Saad, "Dynamic state estimation of a doubly fed induction generator based on a comprehensive nonlinear model", in: Simul. Model. Pract. Theory, vol. 69, pp. 92?112, Dec. 2016.

[21] Divya G Pillai, A. Vivek and V. Srikanth, "Non-linear state estimation of PMSM using derivative-free and square-root Cubature Kalman Filter", in: International Conference on Intelligent Computing, Instrumentation and Control Technologies (ICICICT), July 2017.

[22] Ienkaran Arasaratnam, "Cubature Kalman Filtering: Theory and Applications,", Ph.D. Thesis, School of Graduate Studies of McMaster University, Hamilton, Ontario 2009.

[23] Yan Sun and Qijun Chen, "Joint estimation of states and parameters of vehicle model using cubature Kalman filter," 2016 IEEE International Conference on Systems, Man, and Cybernetics (SMC), Budapest, 2016, pp. 000977-000982, Oct. 2016.

[24] Gopinath G. R. and S. P. Das, "Speed and position sensorless control of Interior Permanent Magnet Synchronous Motor using Square-root Cubature Kalman filter with joint parameter estimation," 2016 IEEE International Conference on Power Electronics, Drives and Energy Systems (PEDES), Trivandrum, 2016, pp. 1-5, Dec. 2016.

[25] H. Pesonen and R. Piché, "Cubature-based Kalman filters for positioning", in: Positioning Navigation and Communication (WPNC), 2010 7th Workshop on , vol., no., pp.45,49, 11-12, March 2010.

[26] Milano, F. "Power System modelling and scripting". ISBN: 978-3-642-13668-9, Springer Publishing Company, Incorporated, 2010.

[27] Ghassempour, H., Miao, Z., Fan, L., Jiang, W. and Manjure, D. "Identification of Synchronous Generator model with Frequency Control Using Unscented Kalman Filter", in: Electric Power Systems Research, Vol. 126, pp. 45-55, Sept. 2015.

[28] Richard Gagnon and Jacques Brochu, "Wind Farm - Synchronous Generator and Full Scale Converter (Type 4) Detailed Model", Mathworks. https://es.mathworks.com/help/physmod/sps/examples/wind-farm-synchronous-generator-and-full-scale-converter-type-4-detailed-model.html. Last visited: July 2019.

[29] S. Julier, "The Scaled Unscented Transformation", in: American Control Conference, 2002. Proceedings of the 2002, IEEE Press, 2002, pp.4555-4559.

[30] J. G. Slootweg, H. Polinder and W. L. Kling, "Initialization of Wind Turbine Models in Power System Dynamics Simulations", in: IEEE Porto Power Tech Proceedings (Cat. No.01EX502), Aug. 2001.

[31] IEC 61400-1, Wind Turbines - Part 1: Design Requirements, International Electrotechnical Commission, Geneva, Switzerland, Tech. Rep., August 2005.